

On the structure of Si(100) surface: Importance of higher order correlations for buckled dimer

Seoin Back, Johan A. Schmidt, Hyunjun Ji, Jiyoung Heo, Yihan Shao, and Yousung Jung

Citation: *The Journal of Chemical Physics* **138**, 204709 (2013); doi: 10.1063/1.4807334

View online: <http://dx.doi.org/10.1063/1.4807334>

View Table of Contents: <http://scitation.aip.org/content/aip/journal/jcp/138/20?ver=pdfcov>

Published by the [AIP Publishing](#)



Re-register for Table of Content Alerts

Create a profile.



Sign up today!



On the structure of Si(100) surface: Importance of higher order correlations for buckled dimer

Seoin Back,¹ Johan A. Schmidt,² Hyunjun Ji,¹ Jiyoun Heo,³ Yihan Shao,⁴
 and Yousung Jung^{1,a)}

¹Graduate School of EEWS (WCU), Korea Advanced Institute of Science and Technology (KAIST),
 Daejeon 305-701, South Korea

²Department of Chemistry, University of Copenhagen, Universitetsparken 5,
 DK-2100 Copenhagen Ø, Denmark

³Department of Biomedical Technology, Sangmyung University, Chungnam 330-720, South Korea

⁴Q-Chem Inc., 5001 Baum Boulevard, Suite 690, Pittsburgh, Pennsylvania 15213, USA

(Received 17 February 2013; accepted 7 May 2013; published online 30 May 2013)

We revisit a dangling theoretical question of whether the surface reconstruction of the Si(100) surface would energetically favor the symmetric or buckled dimers on the intrinsic potential energy surfaces at 0 K. This seemingly simple question is still unanswered definitively since all existing density functional based calculations predict the dimers to be buckled, while most wavefunction based correlated treatments prefer the symmetric configurations. Here, we use the doubly hybrid density functional (DHDF) geometry optimizations, in particular, XYGJ-OS, complete active space self-consistent field theory, multi-reference perturbation theory, multi-reference configuration interaction (MRCI), MRCI with the Davidson correction (MRCI + Q), multi-reference average quadratic CC (MRAQCC), and multi-reference average coupled pair functional (MRACPF) methods to address this question. The symmetric dimers are still shown to be lower in energy than the buckled dimers when using the CASPT2 method on the DHDF optimized geometries, consistent with the previous results using B3LYP geometries [Y. Jung, Y. Shao, M. S. Gordon, D. J. Doren, and M. Head-Gordon, *J. Chem. Phys.* **119**, 10917 (2003)]. Interestingly, however, the MRCI + Q, MRAQCC, and MRACPF results (which give a more refined description of electron correlation effects) suggest that the buckled dimer is marginally more stable than its symmetric counterpart. The present study underlines the significance of having an accurate description of the electron-electron correlation as well as proper multi-reference wave functions when exploring the extremely delicate potential energy surfaces of the reconstructed Si(100) surface. © 2013 AIP Publishing LLC. [<http://dx.doi.org/10.1063/1.4807334>]

I. INTRODUCTION

The Si (100) surface has been a subject of both experimental and theoretical studies for many decades because of its chemical properties and its use in the production of semiconductors.^{1–8} With the size of semiconductor devices decreasing, an accurate understanding of its surface becomes more important. Although many theoretical and experimental studies have been reported, it is still controversial whether the surface is preferentially symmetric or buckled at low temperatures (≤ 100 K) where entropic effects are minor.

From the experimental point of view, the configuration of silicon (100) surface has been an interesting question after Schlier and Farnsworth first reported the dimerizing character of two silicon atoms on the silicon (100) surface.⁹ Spectroscopy and STM experiments suggested that the most stable configuration of silicon (100) surface around 100 K is the $c(4 \times 2)$ arrangement in buckled structure.^{10–13} In 2000, however, the STM and AFM measurements indicated the $p(2 \times 1)$ symmetric image below 80 K.^{6,14–16} Also, LEED measurements below 40 K reported the same structural

change.¹⁷ However, the latter symmetric structures were attributed to the tip-surface interaction in STM that modifies the image from buckled dimers to symmetric, and it seems to be a consensus that the most stable dimer configuration at low temperatures is the buckled $c(4 \times 2)$ arrangement. Another AFM study at 5 K and LEED study below 40 K also suggested the buckled $c(4 \times 2)$ arrangement as the ground state.¹⁴

In theoretical literature, generally, Hartree-Fock (HF), density functional theory (DFT), and quantum Monte Carlo (QMC) predicted the buckled structure to be the lowest energy minimum, while the second order perturbation theory (MP2), multi-configurational self-consistent field (MC-SCF), multi-reference configuration interaction (MRCI), and multi-reference second order perturbation theory (MRMP2) optimizations suggested the symmetric structure to be the global minimum.^{18–26} The CCSD(T) and MRMP2 geometry optimizations for one dimer Si-cluster (Si_2H_{12}) have predicted its structure to be symmetric.²² A recent study using the unrestricted density functional theory (UDFT) with B3LYP functional showed that both symmetric and buckled minima exist, although the energy of buckled configuration was marginally lower than that of the symmetric by 1.40 kcal/mol per dimer for a three-dimer cluster model.²⁵

^{a)} Author to whom correspondence should be addressed. Electronic mail: ysjn@kaist.ac.kr

A more recent occupation restricted multiple active space (ORMAS) study of cluster models for silicon (100) surface also suggested that the distances between dimers are too far to cause the interdimer interactions, which would make the symmetric structure the ground state.²⁷ Lampart and co-workers applied various wavefunction based multi-reference calculations on the Si_2H_4 and Si_7H_8 cluster models. In their study, CASPT3, multi-reference average quadratic CC (MRAQCC), and MRACPF calculations favor the buckled structure by 1.1–1.4 kcal/mol per dimer. They suggested that the dynamic correlation effect not covered in CASPT2 calculation is critical to explore relative energetics of symmetric and buckled structure of Si (100) surface.²⁸

Since there has been no consensus on the lowest energy surface structure between density functional vs. correlated wave function-based calculations, in this paper, we revisited the structure of Si (100) surface using the latest density functional, XYGJ-OS,²⁹ that approaches the chemical accuracy of 1 kcal/mol in predicting the reaction energies and activation barriers and also gives geometries comparable to CCSD(T).³⁰ With the help of XYGJ-OS analytic gradient recently developed in our group,³⁰ in this work we perform the geometry optimization for one-, two-, and three-dimer cluster models of Si (100) using XYGJ-OS. It is also important to emphasize that, although XYGJ-OS shows a promising accuracy for various molecular properties, silicon dimers have significant diradical character with $\sim 35\%$ of electrons occupying the lowest unoccupied molecular orbitals (LUMO).²⁴ Since XYGJ-OS is not guaranteed to describe multi-reference character by its construction, the effect of including multi-reference character should be assessed. For this purpose, complete active space self-consistent field (CASSCF), CASPT2, MRCI(+Q), MRAQCC, and MRACPF energies are calculated for XYGJ-OS optimized dimers. These values are compared with corresponding single-reference methods, HF, MP2, CI(+Q), AQCC, and ACPF, to investigate how the multi-reference character affects relative energetics. In this paper, we use CI to refer to CI singles and doubles (CISD).

This paper is organized as follows: Sec. II describes doubly hybrid density functional calculations and results, while Sec. III describes the wave functions based single- and multi-reference calculations and results, and finally Sec. IV gives a summary of our findings.

II. DOUBLY HYBRID DENSITY FUNCTIONAL CALCULATIONS

One- (Si_9H_{12}), two- ($\text{Si}_{15}\text{H}_{16}$), and three-dimer ($\text{Si}_{20}\text{H}_{21}$) cluster models were used to represent the structure of the Si (100) surface. The XYGJ-OS geometry optimization was performed with the 6-311+G(3df,2p) basis, starting from (U)B3LYP/6-31G(d) optimized geometries (see Ref. 25). Using these structures we calculated single-point energies for three additional doubly hybrid density functionals (DHDFs): B2PLYP,³¹ $\omega\text{B97X-2}$,³² and XYG3.³³ All DHDF calculations were performed using Q-CHEM.³⁴ The XYGJ-OS/6-311+G(3df,2p) optimized structures were also used as starting points for the multi-reference calculations described in Sec. III.

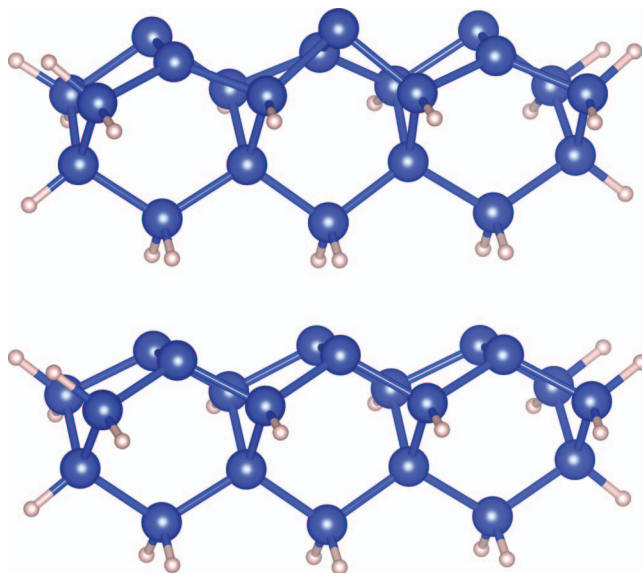


FIG. 1. Three-dimer cluster models ($\text{Si}_{20}\text{H}_{21}$). Upper shows the buckled structure and lower shows the symmetric structure, both optimized at XYGJ-OS/6-311+G(3df,2p).

According to Yang and Kang's work, choice of dimer size and geometric constraints is of significance in describing potential energy surface of silicon dimers.³⁵ A single dimer cluster model is not large enough to obtain correct ground state energies and geometries, while two- and three-dimer cluster models showed a good agreement with the five-layer slab model.^{35,36} Following this conclusion, we optimized up to three-dimer cluster model without any constraints. Figures 1(a) and 1(b) represent buckled and symmetric structure of 3-dimer cluster models ($\text{Si}_{20}\text{H}_{21}$) used in our study.

The XYGJ-OS energy expression involves Kohn-Sham orbitals, which can either be generated using a spin-restricted approach (B3LYP) or alternatively a spin-unrestricted approach (UB3LYP) (Table I). Table I summarizes the energy difference between the restricted and unrestricted approach. All DHDF calculations show that restricted solutions are more stable than unrestricted solutions. Our earlier study of the silicon dimers found the UB3LYP solution to indeed exist and be lower in energy than the B3LYP solution, the spin-unrestricted solution was, therefore, preferred in a variational sense.²⁵ However, in the present study we find that using spin-restricted Kohn-Sham orbitals yields a lower XYGJ-OS energy when additionally considering the perturbative correlation effects. The same behavior was observed for other DHDFs considered here. We, therefore, used spin-restricted Kohn-Sham orbitals.

TABLE I. Energy differences between the spin-restricted and spin-unrestricted solutions, along with $\langle S^2 \rangle$ values for the unrestricted solutions. Calculations are performed with four DHDFs/6-311+G(3df,2p) on the B3LYP optimized symmetric geometry. Positive ΔE means the restricted solution is more stable ($\Delta E_{R \rightarrow U} = E_{\text{unrestricted}} - E_{\text{restricted}}$).

	B2PLYP	$\omega\text{B97X-2}$	XYGJ-OS	XYG3	(U)B3LYP ²⁵
$\Delta E_{R \rightarrow U}$ (kcal/mol)	6.10	5.76	5.04	4.25	-2.01
$\langle S^2 \rangle$	1.42	1.64	0.77	0.77	0.81

TABLE II. The energy difference per dimer between the buckled and symmetric configurations ($\Delta E/\text{dimer}$) calculated using various DHDFs on the XYGJ-OS/6-311+G(3df,2p) optimized geometries. Values in parentheses are based on the single point DHDFs/6-311+G(3df,2p) calculations using the (U)B3LYP optimized geometry in Ref. 25 ($\Delta E = E_{\text{sym}} - E_{\text{buck}}$).

	$\Delta E/\text{dimer}$ (kcal/mol)				
	B2PLYP	ω B97X-2	XYGJ-OS	XYG3	(U)B3LYP ²⁵
1-dimer	0.00 (0.00)	0.00 (0.00)	0.00 (0.00)	0.00 (0.00)	0.05
2-dimer	1.00 (1.49)	1.45 (2.17)	0.42 (0.72)	0.62 (0.93)	0.74
3-dimer	1.84 (2.21)	3.66 (3.03)	1.49 (1.39)	2.27 (1.63)	1.40

Table II shows the energy difference between the buckled and symmetric structure per dimer for XYGJ-OS and other DHDFs for one-, two-, and three-dimers at the XYGJ-OS/6-311+G(3df,2p) optimized geometry. We also included the single-point DHDF/6-311+G(3df,2p) energy calculations on the previous (U)B3LYP/6-31G(d) geometries.²⁵ Positive value means that the buckled structure is lower in energy. Like most existing DFT results, DHDFs favor the buckled structure. As the number of dimers increases, the buckled structure becomes more stable compared to the symmetric structure, indicating significant inter-dimer interactions within these density functionals. Although all DHDFs calculations show the similar trend, for XYGJ-OS and XYG3, increasing the dimer size from two to three increases the relative stability of the buckled structure by a factor of 4. Table II also shows a geometry dependence (XYGJ-OS vs. B3LYP geometries) of the relative stability up to 0.64 kcal/mol per dimer.

III. WAVE FUNCTION BASED CALCULATIONS (SINGLE- AND MULTI-REFERENCE)

The DHDFs used in this study were not designed with static electron-electron correlation in mind. It is, therefore, essential to investigate the effect of the static correlation with methods, which, by design, include this type of correlation. We investigated six multi-reference methods, which are all capable of describing static correlation. The corresponding single reference methods (HF, MP2, CISD, CISD+Q, AQCC, and ACPF) were also investigated which made it possible to isolate the effect having a multi-reference solution. The single reference methods generally form a hierarchy (HF \ll MP2 < CISD < AQCC < ACPF)^{37,38} in terms of their ability to describe dynamic electron-electron correlation. A series of benchmarks against FCI found a similar hierarchy (MRCI < MRAQCC < MRACPF)³⁸ for the multi-reference methods. MRCI here implies MRCI singles and doubles, i.e., MRCISD.

The CASSCF^{39,40} calculations were performed as follows: The one-dimer calculations were carried out without the use of spatial symmetry and with 2 active electrons in 2 orbitals (the HOMO and LUMO). The two-dimer calculations were carried out in the C_2 spatial symmetry and with 4 active electrons in 4 orbitals (from HOMO - 1 to LUMO + 1), while the three-dimer calculations were carried out in the C_s spatial symmetry and with 6 active electrons in 6 orbitals (from HOMO - 2 to LUMO + 2). All orbitals below these levels were either “frozen” (not optimized beyond SCF) or “closed” (optimized but with occupation fixed to 2). The

multi-reference Rayleigh Schrödinger 2nd order perturbation theory (CASPT2)⁴¹ calculations and MRCI^{42,43} calculations, MRAQCC,⁴⁴ and multi-reference average coupled pair functional (MRACPF)⁴⁴⁻⁴⁶ calculations were performed using the CASSCF orbitals and using the CASSCF wavefunction as reference. The MRCI energies were corrected using the Davidson correction⁴⁷ (MRCI + Q) to approximately take into account higher excitations. All single- and multi-reference wavefunction calculations were carried using MOLPRO.⁴⁸

The core orbitals were frozen in CASSCF and CASPT2 calculations. The single- and multi-reference CI, CI + Q, AQCC, and ACPF calculations were in all cases restricted to excitations from no more than 32 orbitals due to limitations in the employed software. This restriction had no consequences for the one-dimer calculations where only the core orbitals were frozen in the MRCI calculations. But for two-dimer and three-dimer MRCI calculations it was necessary to freeze additional 8 and 23 orbitals besides the core orbitals, respectively.

The one-dimer and two-dimer calculations were carried out using the 6-311+G(3df,2p) orbital basis set, while the 3-dimer calculations were performed using a mixed basis where the top layer Si atoms were described using 6-311+G(3df,2p) and all other atoms were described using 6-31G*.

Table III shows the $\Delta E/\text{dimer}$ for one-, two-, and three-dimer systems derived using HF, MP2, CI(+Q), AQCC, ACPF methods, while Table IV shows the $\Delta E/\text{dimer}$ for one-, two-, and three-dimer systems derived using the corresponding multi-reference methods.

A direct comparison of Tables III and IV reveals the following trends: (a) The inclusion of static electron-electron correlation (i.e., going from single-reference to multi-reference) preferentially stabilizes the symmetric configuration. (b) The inclusion of dynamic electron-electron correlation preferentially stabilizes the buckled configuration. (c) The buckled configuration is preferentially stabilized when increasing the number of dimers.

TABLE III. Single-reference relative energies evaluated on the XYGJ-OS/6-311+G(3df,2p) optimized geometries. Negative values mean that the symmetric structure is lower in energy than the buckled structure ($\Delta E = E_{\text{sym}} - E_{\text{buck}}$).

	HF	MP2	CI	CI+Q	AQCC	ACPF
1-dimer	0.00	0.00	0.00	0.00	0.00	0.00
2-dimer	2.82	-0.76	2.34	1.79	1.10	2.72
3-dimer	3.91	1.63	4.22	4.08	3.27	3.22

TABLE IV. Multi-reference relative energies (see text for details) evaluated on the XYGJ-OS/6-311+G(3*df*,2*p*) optimized geometries. Negative values mean that the symmetric structure is lower in energy than the buckled structure. Values in parentheses are based on (U)B3LYP optimized geometries in Ref. 24 ($\Delta E = E_{\text{sym}} - E_{\text{buck}}$).

	CASSCF	CASPT2	MRCI	MRCI+Q	MRAQCC	MRACPF
1-dimer	-0.01	-0.02	-0.01	-0.01	0.00	0.00
2-dimer	-4.08	-1.72	-2.30 (-2.91)	-1.23 (-1.56)	-0.45	-0.22
3-dimer	-4.34	-2.57	-1.16	0.54	1.50	1.80

Trend (a) can be understood by considering the leading coefficients of the MCSCF wavefunctions. For the symmetric configuration the leading coefficients are smaller than for the buckled configurations showing that the symmetric configurations have more of a multi-reference character. Static correlation should, therefore, not be neglected when investigating, whether the Si surface is symmetric or buckled.

The present multi-reference calculations have two main limitations. The first is the relatively small size of the employed orbital basis. The second limitation is the required freezing valence orbitals in the CI, AQCC, and ACPF calculations. The effect of these limitations and the subsequent reliability of the wavefunction-based calculations are discussed below.

The large size of the three-dimer system made the calculations using a pure 6-311+G(3*df*,2*p*) basis set infeasible. A mixed basis was, therefore, employed instead. Test calculations for the 2-dimer system revealed that the mixed basis gave results in fair agreement with pure 6-311+G(3*df*,2*p*) results (deviations of up to 0.7 kcal/mol was seen for $\Delta E/\text{dimer}$ for the two basis sets where the mixed basis made $\Delta E/\text{dimer}$ more negative in MRCI and MRCI + Q calculations). We, therefore, believe that the present three-dimer results are fair estimates for (hypothetical) three-dimer results obtained using a pure 6-311+G(3*df*,2*p*) basis.

As described above, it was necessary to freeze some of the valence orbitals in the CI, AQCC, and ACPF calculations. The effect of this additional freezing of orbitals was quantified through CASPT2 calculations with and without freezing of valence orbitals. The difference in $\Delta E/\text{dimer}$ for two approaches was found to be 1.3 kcal/mol, where freezing valence orbitals made $\Delta E/\text{dimer}$ less negative. Incidentally, the use of mixed basis for 3-dimer (making $\Delta E/\text{dimer}$ more negative) and the use of additional freezing of the valence orbitals (making $\Delta E/\text{dimer}$ less negative) showed opposite trends, potentially allowing for a fortuitous cancellation of errors. The present study, nonetheless, clearly suggests the critical importance of higher-order dynamic correlation effects to definitively determine the relative stability of symmetric vs. buckled Si dimers.

The CASSCF method mostly captures static electron correlation. The MRCI method improves on the CASSCF method by capturing dynamic correlation by considering singles and doubles excitations from the reference into the virtuals. The MRCI + Q method seeks to additionally improve on the MRCI method by approximately accounting for higher excitations. The three methods, therefore, form a hierarchy of increasing dynamic electron correlations. In all cases, the $\Delta E/\text{dimer}$ becomes less negative (and even positive for the

3-dimer) as more dynamic electron correlation is included in the calculations. The results of MRAQCC and MRACPF, known to capture most of electron-electron dynamic correlation, also showed that including dynamic correlation stabilizes the buckled structure. The increased natural orbital occupation numbers of 3-dimer symmetric (1.72) and buckled structure (1.83) of the XYGJ-OS geometries with respect to ORMAS symmetric structure (1.66) indicates the importance of an inter-dimer interaction.⁴⁹

Consider the MRCI, MRCI + Q, MRAQCC, and MRACPF results for the two- and three-dimer systems: As the size of the system is increased (from two to three dimers) the energy becomes less negative (MRCI) and even positive (MRCI + Q, MRACPF, and MRAQCC) indicating that increasing the systems favors the buckled configuration. Interestingly, a similar trend was observed in the DFT calculations for two, three, and four dimers.²⁵ The CASPT2 calculations show an opposite trend. We also note that the MRCI (+Q) calculations on (U)B3LYP geometries yield almost same results, showing a weak geometry dependence between (U)B3LYP and XYGJ-OS in the present case.

IV. CONCLUSIONS

With the recently developed XYGJ-OS gradient codes, we have revisited the relative stability of symmetric vs. buckled dimers on the reconstructed Si(100) surfaces. XYGJ-OS geometry optimization prefers the buckled dimer to be the global minimum like all other DFT calculation results. Single point calculations using the other flavors of doubly hybrid functional, i.e., B2PLYP, ω B97X-2, and XYG3, yield the same trend although the quantitative relative energies differ by up to 2 kcal/mol per dimer. Proper inclusion of multi-reference character for the diradicaloid Si-Si dimers as well as the dynamic correlation effects in CASPT2 calculations, however, suggest that the symmetric dimers are lower in energy than the buckled configurations. Interestingly, however, including more refined dynamic correlation in MRCI + Q, MRAQCC, and MRACPF place the buckled structure to be lower in energy. The present study clearly indicates a significance of higher-order dynamic correlations as well as appropriate multi-reference wavefunctions in exploring the extremely shallow potential energy surfaces of the reconstructed Si (100) surface.

ACKNOWLEDGMENTS

We are pleased to acknowledge the support of Basic Science Research (2010-0023018), WCU (R-31-2008-000-10055-0) programs, EDISON (2012M3C1A6035359) funded

by the Ministry of Education, Science, and Technology of Korea, and generous supercomputing time from KISTI. Y.S. acknowledges financial support from NIH through SBIR Grant No. GM096678.

- ¹P. Kratzer, B. Hammer, and J. No, *Phys. Rev. B* **51**, 13432 (1995).
- ²R. A. Wolkow, *Phys. Rev. Lett.* **68**, 2636 (1992).
- ³J. T. Yates and H. N. Waltensburg, *Chem. Rev.* **95**, 1589 (1995).
- ⁴D. Badt, H. Wengelnic, and H. Neddermeyer, *J. Vac. Sci. Technol. B* **12**, 2015 (1994).
- ⁵W. A. Goddard III and T. McGill, *J. Vac. Sci. Technol.* **16**, 1308 (1979).
- ⁶T. Yokoyama and K. Takayanagi, *Phys. Rev. B* **61**, R5078 (2000).
- ⁷Y. Jung, C. H. Choi, and M. S. Gordon, *J. Phys. Chem. B* **105**, 4039 (2001).
- ⁸Y. Jung and M. S. Gordon, *J. Am. Chem. Soc.* **127**, 3131 (2005).
- ⁹R. Schlier and H. Farnsworth, *J. Chem. Phys.* **30**, 917 (1959).
- ¹⁰H. Tochiwara, T. Amakusa, and M. Iwatsuki, *Phys. Rev. B* **50**, 12262 (1994).
- ¹¹H. Shigekawa, K. Miyake, M. Ishida, and K. Hata, *Jpn. J. Appl. Phys., Part 2* **36**, L294 (1997).
- ¹²H. Shigekawa, K. Hata, K. Miyake, M. Ishida, and S. Ozawa, *Phys. Rev. B* **55**, 15448 (1997).
- ¹³K. Hata, M. Ishida, K. Miyake, and H. Shigekawa, *Appl. Phys. Lett.* **73**, 40 (1998).
- ¹⁴T. Uozumi, Y. Tomiyoshi, N. Suehira, Y. Sugawara, and S. Morita, *Appl. Surf. Sci.* **188**, 279 (2002).
- ¹⁵K. Hata, S. Yoshida, and H. Shigekawa, *Phys. Rev. Lett.* **89**, 286104 (2002).
- ¹⁶M. Ono, A. Kamoshida, N. Matsuura, E. Ishikawa, T. Eguchi, and Y. Hasegawa, *Phys. Rev. B* **67**, 201306 (2003).
- ¹⁷M. Matsumoto, K. Fukutani, and T. Okano, *Phys. Rev. Lett.* **90**, 106103 (2003).
- ¹⁸M. S. Gordon, J. R. Shoemaker, and L. W. Burggraf, *J. Chem. Phys.* **113**, 9355 (2000).
- ¹⁹S. B. Healy, C. Filippi, P. Kratzer, E. Penev, and M. Scheffler, *Phys. Rev. Lett.* **87**, 016105 (2001).
- ²⁰J. R. Shoemaker, L. W. Burggraf, and M. S. Gordon, *J. Phys. Chem. A* **103**, 3245 (1999).
- ²¹M. S. Gordon, J. R. Shoemaker, and L. W. Burggraf, *J. Chem. Phys.* **113**, 9355 (2000).
- ²²R. M. Olson and M. S. Gordon, *J. Chem. Phys.* **124**, 081105 (2006).
- ²³J. Hess and D. Doren, *J. Chem. Phys.* **113**, 9353 (2000).
- ²⁴Y. Jung, Y. Akinaga, K. D. Jordan, and M. S. Gordon, *Theor. Chem. Acc.* **109**, 268 (2003).
- ²⁵Y. Jung, Y. Shao, M. S. Gordon, D. J. Doren, and M. Head-Gordon, *J. Chem. Phys.* **119**, 10917 (2003).
- ²⁶B. Paulus, *Surf. Sci.* **408**, 195 (1998).
- ²⁷L. Roskop and M. S. Gordon, *J. Phys. Chem. A* **114**, 8817 (2010).
- ²⁸W. Lampart, D. Schofield, R. Christie, and K. Jordan, *Mol. Phys.* **106**, 1697 (2008).
- ²⁹I. Y. Zhang, X. Xu, Y. Jung, and W. A. Goddard III, *Proc. Natl. Acad. Sci. U.S.A.* **108**, 19896 (2011).
- ³⁰H. Ji, Y. Shao, W. A. Goddard, and Y. Jung, *J. Chem. Theory Comput.* **9**, 1971 (2013).
- ³¹S. Grimme, *J. Chem. Phys.* **124**, 034108 (2006).
- ³²J. D. Chai and M. Head-Gordon, *J. Chem. Phys.* **131**, 174105 (2009).
- ³³Y. Zhang, X. Xu, and W. A. Goddard, *Proc. Natl. Acad. Sci. U.S.A.* **106**, 4963 (2009).
- ³⁴Y. Shao, L. F. Molnar, Y. Jung, J. Kussmann, C. Ochsenfeld, S. T. Brown, A. T. B. Gilbert, L. V. Slipchenko, S. V. Levchenko, and D. P. O'Neill, *Phys. Chem. Chem. Phys.* **8**, 3172 (2006).
- ³⁵C. Yang and H. C. Kang, *J. Chem. Phys.* **110**, 11029 (1999).
- ³⁶E. Penev, P. Kratzer, and M. Scheffler, *J. Chem. Phys.* **110**, 3986 (1999).
- ³⁷F. Jensen, *Introduction to Computational Chemistry* (Wiley, New York, 2007), p. 184.
- ³⁸P. G. Szalay, *Recent Advances in Coupled-Cluster Methods*, edited by R. J. Bartlett (World Scientific, Singapore, 1997), Vol. 3, pp. 81–123.
- ³⁹P. J. Knowles and H.-J. Werner, *Chem. Phys. Lett.* **115**, 259 (1985).
- ⁴⁰H. J. Werner and P. J. Knowles, *J. Chem. Phys.* **82**, 5053 (1985).
- ⁴¹P. Celani and H.-J. Werner, *J. Chem. Phys.* **112**, 5546 (2000).
- ⁴²H. J. Werner and P. J. Knowles, *J. Chem. Phys.* **89**, 5803 (1988).
- ⁴³P. J. Knowles and H.-J. Werner, *Chem. Phys. Lett.* **145**, 514 (1988).
- ⁴⁴P. G. Szalay and R. J. Bartlett, *Chem. Phys. Lett.* **214**, 481 (1993).
- ⁴⁵H.-J. Werner and P. J. Knowles, *Theor. Chim. Acta* **78**, 175 (1990).
- ⁴⁶R. J. Gdanitz and R. Ahlrichs, *Chem. Phys. Lett.* **143**, 413 (1988).
- ⁴⁷S. R. Langhoff and E. R. Davidson, *Int. J. Quantum Chem.* **8**, 61 (2004).
- ⁴⁸H.-J. Werner, P. Knowles, R. Lindh, F. Manby, M. Schütz *et al.*, MOLPRO, version 2006.1, a package of *ab initio* programs, 2006, see <http://www.molpro.net>.
- ⁴⁹See supplementary material at <http://dx.doi.org/10.1063/1.4807334> for XYGJ-OS geometries and the natural orbital occupation numbers.